XXXX XXX

Estimation of Motion Statistics from Statistics of Received Power in Low-Power IoT Sensing Nodes

Waltenegus Dargie, Senior Member, IEEE
Faculty of Computer Science, Technische Universität Dresden, 01062 Dresden, Germany

Manuscript received July 7, 2024; revised September 23, 2024.

Abstract—Low-power IoT sensing nodes can be embedded into various physical environments to monitor vital parameters. Some of these environments impose rough and extreme operation conditions, severely limiting the performance of these nodes. Modeling these environments is vital to make the nodes adaptive. In this paper, we propose a model to estimate the complex motion of nodes deployed on the surface of different water bodies. The model relies on received power statistics only. Experiment results confirm that the model is reliable, achieving an estimation accuracy of 93%.

Index Terms—3D water motion, IMU, IoT, MS estimation, received power, RSSI, wireless sensor networks

I. INTRODUCTION

Low-power and wireless IoT sensing nodes can be deployed in various physical environments to monitor vital parameters [1]. Some of the deployment environments are not amenable to stable and reliable operations, subjecting the nodes to strong motion, thereby significantly interfering with their operation. Modelling these environments and their effects on the sensing nodes is vital to achieve different objectives, including transmission power adaptation, developing path loss models, and estimation of performance and operation lifetime. Moreover, associating environmental aspects with performance can be useful for assessing the authenticity of the origin of data.

The aim of this paper is to achieve this goal. We deployed low-power IoT sensing nodes on the surface of different water bodies to monitor water quality. The performance of these nodes, particularly, the quality of the wireless links they established, was considerably affected by the motion of water. Each of these nodes integrated two types of low-power radios operating in different frequency bands (2.4 GHz and 868 MHz) and supporting different transmission ranges (100 m vs 4 Km) as well as transmission rates (250 kbps vs. 40 kbps). Because of their inherent characteristics, the water bodies exhibited different motion patterns and affected the quality of the wireless links differently. In order to investigate the effect of motion on the link quality, we integrated inertial sensors (3D accelerometers and 3D gyroscopes) with the sensing nodes. As the first contribution of this paper, we propose a statistical model to express the 3D motion of the water surfaces in terms of a one-dimensional link quality metric, the RSSI. The model is at once accurate and efficient. It achieves an estimation accuracy exceeding on average 93%. This is rather remarkable considering the fact that the model relies on an unreliable link quality metric and its computational cost is modest, requiring no matrix inversion. As a second contribution of the paper, through extensive field deployments and experiments, we validate the reliability of our model.

The remaining part of the paper is organized as follows. In Section II we review papers which are related to our work. In Section III, we briefly describe the deployment scenarios wherein we conducted extensive experiments. In Section IV, we present our model and derive the model parameters using MS estimation. In Section V we evaluate our model and present quantitative results. Finally, in Section VI, we provide concluding remarks and outline future work.

Corresponding author: W. Dargie (e-mail: waltenegus.dargie@tu-dresden.de).

Associate Editor: XXX
Digital Object Identifier XXXX

II. RELATED WORK

Modeling the motion of the surface of water is useful for a wide range of applications [2], [3]. In the context of maritime and cellular communications (5G networks) various path loss and water motion models have been proposed to characterise near sea-surface wireless channels. Some of these models build on Pierson–Moskowitz spectrum [4], [5], a condition in which water waves attain equilibrium with a steadily blowing wind. In [6], a model is proposed to estimate the maximum wave-height occurring between two communicating wireless sensor nodes deployed on the surface of an ocean. The maximum wave-height statistics are used to determine the probability of LoS blockage. In [7] a "fluctuating" 2-ray fading model, first proposed by Romero et al. [8], is employed to account for random amplitude variations of sea waves. In [9], a 3-ray path loss model is proposed to account for reflection from sea surface and refraction caused by evaporation duct. In [10] a model characterizing seawater-to-air optical channels is proposed. The model takes into consideration pitching angle (modelled by Beckmann distribution), attenuation (Beer-Lambert) and underwater turbulence (Lognormal. The above models aim to estimate received power statistics in deployments involving rough water surfaces; our approach complements them by addressing the inverse problem, i.e., estimating motion statistics from received power statistics.

Eltner et al. [11] propose a model based on structure-from-motion (a process of estimating the 3D structure of a scene from a set of 2D images) and multi-media photogrammetry to estimate surface flow velocity and water discharge in rivers. The model relies on images taken by a UAV and an additional static camera. Though the authors report an impressive accuracy reaching 96%, the model also suffers from a high estimation variance. A work closer to ours is the one propose by Amaechi et al. [12]. In this work, the authors endeavour to model the motion of different marine structures – dynamic loading and offloading buoys (Catenary Anchor Leg Moorings) and ocean monitoring buoys. The model relies on two Ultra-High Definition underwater cameras and an underwater motion sensor. The latter

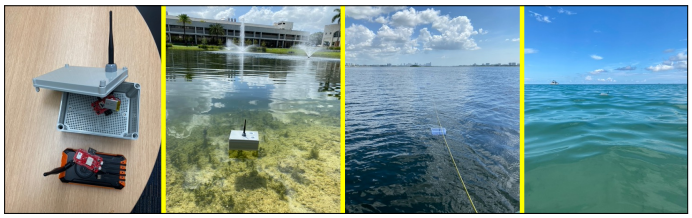

Fig. 1. The deployment of IoT sensing nodes on the surface of different water bodies (lake, North Biscayne Bay, Miami South Beach, and Crandon Beach).

consists of a 10-axis IMU integrating an accelerometer, a gyroscope, an angle measurement, a magnetometer, and a barometer. These systems were connected to an external system via an underwater Bluetooth. The data collected from these sensors are fused together and transformed into three linear equations to characterise the motion of the marine structure: (1) wave frequency versus period, (2) surge response, and (3) heave response. Unfortunately, the authors do not discuss the accuracy as well as the complexity of their model. The preceding approaches complex sensing setups, large-scale deployments, and/or advanced signal processing which incur appreciable communication and processing cost. By contrast, our approach is lightweight, at first requiring acceleration and received power statistics. Once the model parameters are determined, it relies only on the statistics of the received power to estimate the motion of the surface of water on which low-power IoT sensing nodes are deployed.

III. BACKGROUND

Between 1 June and 31 August 2023, we deployed networks of low-power IoT nodes on the surfaces of different water bodies: A small lake on the main campus of Florida International University (FIU), North Biscayne Bay in South Florida, Miami South Beach, and Crandon Beach, Miami. Some of the deployments took place at the time when the State of Florida was significantly affected by Hurricane Idalia, a Category 4 hurricane.[1] Fig. 1 displays a snapshot of our prototypes and deployments. The bodies of water have different characteristics as well as temporal and seasonal motion patterns. The nodes established multi-hop networks through peer-to-peer neighbour discovery and periodically exchanged packets. Locally, the nodes stored the 3D acceleration they experienced along with timestamps. Likewise, when nodes received a packet, they stored the received power (RSSI) and other link quality metrics along with timestamps.

Fig. 2 shows the change in the received power and the associated change in the linear acceleration (the acceleration along the x- and z-axes are shown) for one of our transmitters. The two low-power radios – CC1200 and CC2538 – integrated into our sensing platform calculated the RSSI as follows: within the bandwidth of each 2 MHz channel (IEEE 802.15.4), the received power corresponding to 8 successive symbols is averaged. Ideally, the mapping from a received power in decibels to an RSSI value is linear, with an accuracy of ± 6 dBm. As can be seen in Fig. 2, the received power appears to have experienced both localized and gradual changes. This reflects the underlying reality. For at the time the measurements were taken, the transmitter node was experiencing translational motion as well as localized oscillations due to a strong north-east wind causing strong

[1]https://www.weather.gov/tae/HurricaneIdalia2023.

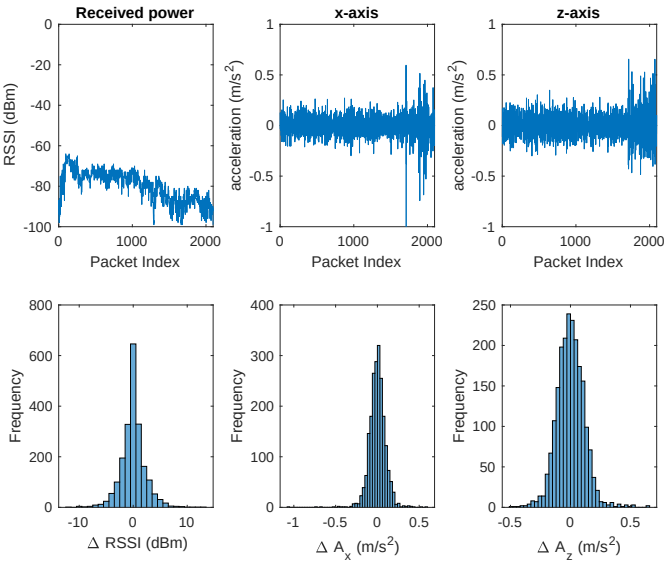

Fig. 2. The relationship between the change in the received power and the linear acceleration a transmitting node experienced on the surface of the Atlantic Ocean. Deployment: Crandon Beach. Radio: CC2538 System-on-Chip.

waves on the Atlantic Ocean. Since the underlying cause of these changes was natural, we expected their distributions to be normal. As can be seen in the figure, the plots of their histograms suggest that they can, indeed, be regarded as normally distributed.

IV. MODEL

In the subsequent discussions we represent random variables with boldface letters and simple values the random variables take, with plane letters. Assuming the existence of a one-to-one relationship between the change in the acceleration ($\mathbf{a}$) and the change in the received power ($\mathbf{r}$), the conditional pdf, $f_{a|r}(a|r)$ provides the complete statistics of the parameters we wish to estimate. The marginal statistics in Fig. 2 suggest that the conditional pdf is jointly normal. The two-dimensional statistics, for instance, should have the following form:[2]

$$f_{a_x,a_z|r}(a_x,a_z|r) = D\ exp\left\{-\left(\frac{1}{2(1-\rho^2)}\right)(X - 2\rho C + Z)\right\} \quad (1)$$

where:

$$X = \frac{(a_x - E[\mathbf{a}_x|r])^2}{\sigma_x^2}$$

$$C = \frac{(a_x - E[\mathbf{a}_x|r])\,(a_z - E[\mathbf{a}_z|r])}{\sigma_x \sigma_z}$$

$$Z = \frac{(a_z - E[\mathbf{a}_z|r])^2}{\sigma_z^2}$$

$$D = \frac{1}{2\pi\sigma_x\sigma_z\sqrt{1-\rho^2}}$$

and ρ, $|\rho| < 1$, is the correlation coefficient of $\mathbf{a}_x$ and $\mathbf{a}_z$. The variances in Equation 1 are the errors we introduce in our estimation of $\mathbf{a}_x$ and $\mathbf{a}_z$ in terms of $\mathbf{r}$.

[2]In order to make the subsequent steps comprehensible, our focus will be on estimating the 2D acceleration only, but one can easily extend the approach to a third-dimension as well.

The one-to-one assumption enables us to deduce the nature of the relationship between the variables from their cumulative distribution functions. If we suppose $0 \leq \mathbf{r} \leq R$ and $0 \leq \mathbf{a} \leq A$, then, $\forall a_j, 0 \leq a_j \leq A$, there is a corresponding $r_i, 0 \leq r_i \leq R$, such that $F_a(a_j) = F_r(r_i)$, from which we have: $a_j = F_a^{-1}(F_r(r_i))$. When $F_a(a)$ and $F_r(r)$ have similar forms, then this implies that the random variables are linearly related [13], in which case, the parameters of Equation 1 can best be determined using Minimum Mean Square estimation. Thus, the error we introduce in expressing the motion (acceleration) a node experiences during transmission is expressed as follows:

$$\begin{aligned} \mathbf{e}_x &= \mathbf{a}_x - \rho_x \mathbf{r}, \\ \mathbf{e}_z &= \mathbf{a}_z - \rho_z \mathbf{r} \end{aligned} \tag{2}$$

In order to determine the optimal ρ_x and ρ_z which minimise the estimation error, we differentiate the mean square errors with respect to these coefficients and set the results to zero:

$$\frac{d}{d\rho_x} E\left\{\mathbf{e}_x^2\right\} = \frac{d}{d\rho_x} E\left\{(\mathbf{a}_x - \rho_x \mathbf{r})^2\right\} = E\left\{(\mathbf{a}_x - \rho_x \mathbf{r})\,\mathbf{r}\right\} = 0 \tag{3}$$

This leads to the following expression:

$$\rho_x = \frac{E\left[\mathbf{a}_x \mathbf{r}\right]}{E\left[\mathbf{r}^2\right]} \tag{4}$$

Similar steps lead to:

$$\rho_z = \frac{E\left[\mathbf{a}_z \mathbf{r}\right]}{E\left[\mathbf{r}^2\right]} \tag{5}$$

With ρ_x and ρ_z in place, we can determine the conditional means in Equation 1:

$$\begin{aligned} E\left[\mathbf{a}_x | r\right] &= \frac{E\left[\mathbf{a}_x \mathbf{r}\right]}{E\left[\mathbf{r}^2\right]} r \\ E\left[\mathbf{a}_z | r\right] &= \frac{E\left[\mathbf{a}_z \mathbf{r}\right]}{E\left[\mathbf{r}^2\right]} r \end{aligned} \tag{6}$$

One of the most interesting aspects of the MS estimation is that the error is orthogonal to the observation, i.e., to $\mathbf{r}$ [13], [14] (ref. also to Equation 3). Hence, expressing the MS error in terms of ρ_x and ρ_z yields:

$$E\left[\mathbf{e}_x^2\right] = R_{xx} - \frac{R_{xr}^2}{R_{rr}} \tag{7}$$

where $R_{xx} = E[\mathbf{a}_x \mathbf{a}_x]$; $R_{xr} = E[\mathbf{a}_x \mathbf{r}]$; and $R_{rr} = E[\mathbf{r}\mathbf{r}]$. Similarly,

$$E\left[\mathbf{e}_z^2\right] = R_{zz} - \frac{R_{zr}^2}{R_{rr}} \tag{8}$$

Finally, the conditional covariance is given as:

$$C_{x,z|r} = E\left[\left(\mathbf{a}_x - \left(\frac{R_{xr}}{R_{rr}}\right)\mathbf{r}\right)\left(\mathbf{a}_z - \left(\frac{R_{zr}}{R_{rr}}\right)\mathbf{r}\right) | \mathbf{r} = r\right] \tag{9}$$

Once again, taking advantage of the orthogonality principle, we ignore the term $\mathbf{r}(t) = r$ in Equation 9 (the error is orthogonal to the data). What remains is the expansion of the error terms, which yields,

$$C_{x,z|r} = R_{xz} - \frac{R_{xr} R_{zr}}{R_{rr}} \tag{10}$$

This completes the specification of the conditional density function. Fig. 3 shows the conditional pdf of the acceleration a transmitting node experienced in South Beach, Miami, Florida.

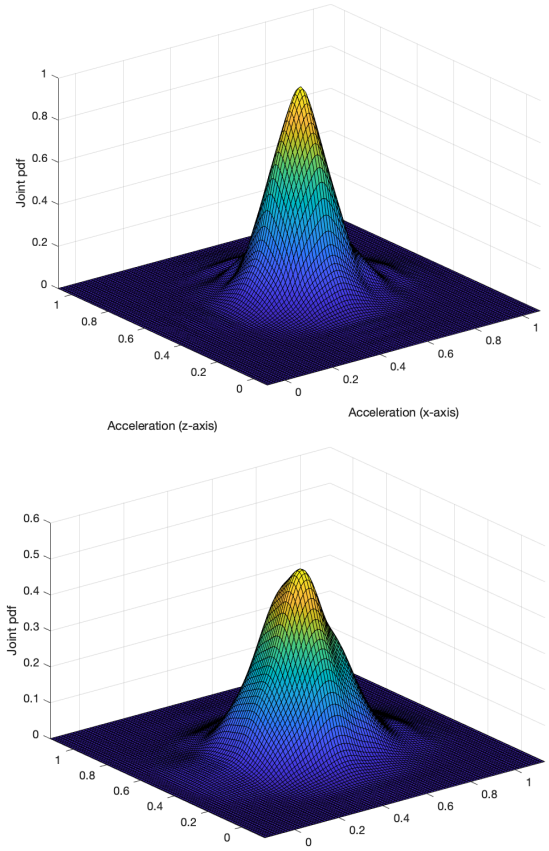

Fig. 3. The conditional pdfs of the 2D acceleration transmitting nodes experienced while communicating. TOP: Miami Crandon Beach. BOTTOM: Miami South Beach.

V. EVALUATION

In order to evaluate the accuracy of our model, we measured (using IMU) as well as estimated (using Equation 6) the change in the acceleration a transmitting node experienced at Miami Crandon Beach and Miami South Beach. For each location-radio pair we performed 5 experiments over a period of 3 months, each experiment lasting about 30 minutes. Then we evaluated the statistics of the two quantities. Fig. 4 compares the histograms of these two quantities. The estimation error statistics are given in Fig. 5. The mean square error statistics were influenced mainly by the motion of water. For the pattern as well as the magnitude of the waves influenced signal propagation and reception, as was discussed in Section II. The water waves at Crandon Beach were short but fast moving, whereas the waves at Miami South Beach were long and large, making them more predictable, as they exhibited a stronger autocorrelation. The average root mean square error, taking into account all the experiments we conducted, was about 7%.

The estimation accuracy our model achieved is either comparable or slightly better than the accuracy reported in Section II. What is appreciable about our models is that it does not require an extra channel, hardware component, or complex setup. The RSSI is a by-product; extracted from data packets. The IMU data we collected were used for training and test purposes. Both these phases are relevant, but typically, the water characteristics change slowly overtime; and updating the model statistics take place at a much longer time interval than the typical duration required to collect representative statistics.

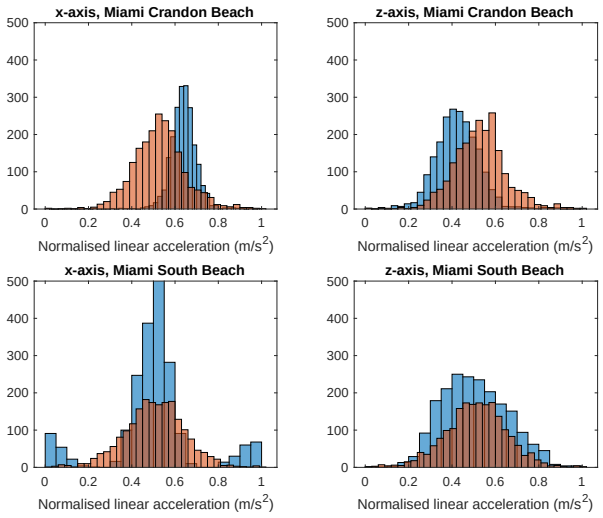

Fig. 4. The histograms of the measured (blue) vs. estimated (red) linear acceleration the wireless sensor nodes experienced on the surface of the Atlantic Ocean. TOP: Miami Crandon Beach. BOTTOM: Miami South Beach.

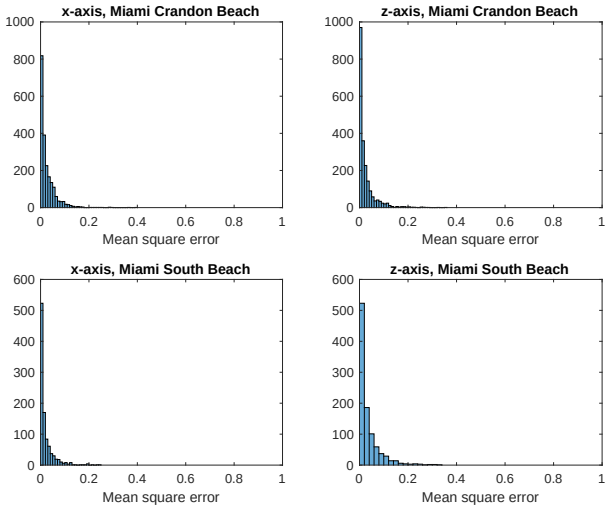

Fig. 5. The histograms of the mean square estimation error for Fig. 4. TOP: Miami Crandon Beach. BOTTOM: Miami South Beach.

The model's accuracy can be greatly improved by using orthogonal or circular antennae, so that the change in the received power can be modelled as a 3-dimensional phenomena which better reflects the 3-dimensional motion of the underlying water surface. Another source of error which does not belong to the model is synchronisation error. In establishing the model parameters, our model presupposes that the inertial measurement unit at the transmitter and the receiver radio are time-synchronised. Due to clock drifts in both systems, however, achieving a more perfect synchronisation requires a more complex and cost-intensive setup than was supported in the present case. Addressing these and similar concerns will be the focus of our future research.

VI. CONCLUSION

In this paper we proposed a model to predict the motion (acceleration) a low-power IoT sensing node experiences when deployed on the surface of different water bodies. We relied on a one-dimensional metric, the RSSI, to estimate the acceleration. The model achieves an estimation accuracy exceeding 93%. Compared to competitive approaches, our model does not require a complex setup or an advanced signal processing. The model's accuracy can be improved by employing orthogonal or circular antennae. A more accurate time synchronisation can also reduce the error arising from low-level clock drifts. Addressing these issues will be the focus of our future research.

REFERENCES

[1] W. Dargie and C. Poellabauer, *Fundamentals of wireless sensor networks: theory and practice*. John Wiley & Sons, 2010.

[2] F. S. Alqurashi, A. Trichili, N. Saeed, B. S. Ooi, and M.-S. Alouini, "Maritime communications: A survey on enabling technologies, opportunities, and challenges," *IEEE Internet of Things Journal*, vol. 10, no. 4, pp. 3525–3547, 2022.

[3] G. Giorgi, R. P. Gomes, J. C. Henriques, L. M. Gato, G. Bracco, and G. Mattiazzo, "Detecting parametric resonance in a floating oscillating water column device for wave energy conversion: Numerical simulations and validation with physical model tests," *Applied Energy*, vol. 276, p. 115421, 2020.

[4] A. Ishimaru, *Electromagnetic wave propagation, radiation, and scattering: from fundamentals to applications*. John Wiley & Sons, 2017.

[5] G. Komen, S. Hasselmann, and K. Hasselmann, "On the existence of a fully developed wind-sea spectrum," *Journal of physical oceanography*, vol. 14, pp. 1271–1285, 1984.

[6] A. Shahanaghi, Y. Yang, and R. M. Buehrer, "Stochastic link modeling of static wireless sensor networks over the ocean surface," *IEEE Transactions on Wireless Communications*, vol. 19, no. 6, pp. 4154–4169, 2020.

[7] J. Wang, H. Zhou, Y. Li, Q. Sun, Y. Wu, S. Jin, T. Q. S. Quek, and C. Xu, "Wireless channel models for maritime communications," *IEEE Access*, vol. 6, pp. 68 070–68 088, 2018.

[8] J. M. Romero-Jerez, F. J. Lopez-Martinez, J. F. Paris, and A. J. Goldsmith, "The fluctuating two-ray fading model: Statistical characterization and performance analysis," *IEEE Transactions on Wireless Communications*, vol. 16, no. 7, pp. 4420–4432, 2017.

[9] L. Yee Hui, F. Dong, and Y. S. Meng, "Near sea-surface mobile radiowave propagation at 5 ghz: measurements and modeling," *Radioengineering*, vol. 23, no. 3, pp. 824–830, 2014.

[10] Y. Ata and K. Kiasaleh, "Performance of optical seawater-to-air wireless links in the presence of seawater pitching angle effect," *IEEE Transactions on Communications*, pp. 1–1, 2024.

[11] A. Eltner, H. Sardemann, and J. Grundmann, "Flow velocity and discharge measurement in rivers using terrestrial and unmanned-aerial-vehicle imagery," *Hydrology and Earth System Sciences*, vol. 24, no. 3, pp. 1429–1445, 2020.

[12] C. V. Amaechi, F. Wang, and J. Ye, "Experimental study on motion characterisation of calm buoy hose system under water waves," *Journal of Marine Science and Engineering*, vol. 10, no. 2, p. 204, 2022.

[13] A. Papoulis and S. Unnikrishna Pillai, *Probability, random variables and stochastic processes*. McGraw-Hill Higher Education (4. edition), 2002.

[14] X.-D. Zhang, *Modern signal processing*. Walter de Gruyter GmbH & Co KG, 2022.